Published in final edited form as:
Mol Imaging Biol. 2011 August ; 13(4): 623–632. doi:10.1007/s11307-010-0397-7.

Quantitating Antibody Uptake *In Vivo*: Conditional Dependence on Antigen Expression Levels

Greg M. Thurber and **Ralph Weissleder***
Center for Systems Biology, Massachusetts General Hospital, Harvard Medical School, Boston, MA 02114

Abstract

Purpose—Antibodies form an important class of cancer therapeutics, and there is intense interest in using them for imaging applications in diagnosis and monitoring of cancer treatment. Despite the expanding body of knowledge describing pharmacokinetic and pharmacodynamic interactions of antibodies *in vivo*, discrepancies remain over the effect of antigen expression level on tumoral uptake with some reports indicating a relationship between uptake and expression and others showing no correlation.

Procedures—Using a cell line with high EpCAM expression and moderate EGFR expression, fluorescent antibodies with similar plasma clearance were imaged *in vivo*. A mathematical model and mouse xenograft experiments were used to describe the effect of antigen expression on uptake of these high affinity antibodies.

Results—As predicted by the theoretical model, under subsaturating conditions, uptake of the antibodies in such tumors is similar because localization of both probes is limited by delivery from the vasculature. In a separate experiment, when the tumor is saturated, the uptake becomes dependent on the number of available binding sites. In addition, targeting of small micrometastases is shown to be higher than larger vascularized tumors.

Conclusions—These results are consistent with the prediction that high affinity antibody uptake is dependent on antigen expression levels for saturating doses and delivery for subsaturating doses. It is imperative for any probe to understand whether quantitative uptake is a measure of biomarker expression or transport to the region of interest. The data provide support for a predictive theoretical model of antibody uptake, enabling it to be used as a starting point for the design of more efficacious therapies and timely quantitative imaging probes.

Keywords

Antibody localization; antigen expression; tumor targeting; binding site barrier; saturation

Introduction

Antibodies are used to treat a variety of cancers, and increasingly, they are being tested as imaging agents for patient selection and monitoring of therapeutic effectiveness[1-3]. These macromolecules are able to specifically bind to a target antigen of interest with high affinity and specificity, blocking signaling receptors and/or recruiting the host immune system to disrupt growth and destroy the cells. Current therapeutic efforts are being made to attach biological toxins or radioisotopes (either directly or in multi-step therapies) to provide additional mechanisms for cancer cell death[4-7]. For imaging, they are being fluorescently

* Corresponding author. rweissleder@mgh.harvard.edu, Simches Research Building, 185 Cambridge St. Boston, MA 02114.

tagged for fluorescence guided surgery[8-11] and radiolabeled for patient selection and monitoring during treatment[12-15]. One problem with these therapies is that they are expensive and only a fraction of patients respond. Ideally, an imaging agent would be able to identify responders prior to the initiation of treatment.

Despite extensive research with these drugs, there is still discrepancy over the effect of the expression level of the target on cells and the uptake *in vivo*. Some reports indicate a correlation between uptake and expression level[1,16,17] as one may intuitively expect. However, other results show no correlation between expression and uptake[18,19] and have implicated vascularization as a better predictor of uptake[20]. It is imperative to understand the conditions under which localization is proportional to antigen expression, otherwise the imaging signal intensity may incorrectly identify the presence or absence of a particular biomarker. This paper seeks to provide a theoretical and experimental basis for understanding these conflicting results.

Given the complexity of targeting tumors in vivo, theoretical modeling becomes essential for isolating the effects of individual parameters. Experimentally, the same antibody can be used to target different tumors with varying expression, but this does not account for tumor spatial and temporal heterogeneity. Likewise, the same tumor can be targeted with antibodies against different antigens with varying expression, but this does not account for differences in antibody pharmacokinetics. The theoretical model can be used to predict the effect of antigen concentration on targeting, ceteris paribus, and the two types of experiments can be compared to this ideal scenario.

In this report, we use a previously developed theoretical model and pharmacokinetic analysis of antibody transport[8,21-24] to describe the conditions under which uptake is predicted to be proportional to expression level and those where it is not. This model describes antibody uptake for cell surface antigens present in solid tumors or liquid tumors (e.g. lymphomas) when the cells are in a vascularized tumor. An experimental xenograft model is used to test the specific hypothesis *in vivo* under controlled conditions. When the tumor is not saturated by antibody, uptake is limited by delivery, more specifically by extravasation from the tumor vasculature. Under saturating conditions, delivery is sufficient to supply antibody for all expressed antigen, and uptake is limited by the number of binding sites. In the latter case, image intensity is proportional to antigen expression levels. These considerations are critical when quantifying localization *in vivo*, since measurements may report the concentration of the biomarker of interest or simply delivery of the probe to the region.

Materials and Methods

Theoretical Model

The theoretical mathematical model to predict the distribution and uptake of antibodies in vascularized tumors and micrometastases has been described previously[8,21-24]. Recently it has been extended to other macromolecules and nanoparticles[25]. Briefly, for a vascularized tumor, a Krogh cylinder setup is used where the plasma concentration in the tumor capillaries follows a biexponential decay. Exchange between the plasma and tumor interstitium is governed by the permeability of the tumor capillaries. Once outside the vessel, the antibody is controlled by diffusion, binding, dissociation, and cellular internalization rates. A prevascular metastasis is modeled as a sphere in a homogeneous normal tissue compartment, where the surrounding concentration is governed by the decaying plasma concentration, normal tissue capillary extravasation rate, and lymphatic drainage rate. Once inside the metastasis, the same diffusion and molecular interaction rates control distribution. It is important to note that while this model predicts the overall antibody

concentration in tumors, it does not assume homogeneous uptake. The low Biot number for macromolecules[24] enables the average uptake to be calculated without explicitly examining the heterogeneous distribution in the tumor. It is also assumed that tumor uptake is not sufficient to affect the plasma concentration (e.g. no TMDD)[26]. The model was used to determine the sensitivity of various parameters in order to ensure measurement of the most influential parameters. For example, plasma clearance (AUC) is expected to have a significant impact on uptake, so the blood half life of both antibodies was measured to verify it was similar for each. On the contrary, for high affinity antibodies (e.g. single digit nanomolar Kd), the affinity is predicted to have little effect on uptake, and this has been shown experimentally[27].

Antibodies

A mouse monoclonal anti-EpCAM antibody (clone# 158206, R&D Systems; Minneapolis, MN) and chimeric anti-EGFR antibody cetuximab (ImClone; Branchburg, NJ) were used for the *in vivo* experiments. The antibodies were labeled with either VivoTag 680 (VT680) fluorophore (Visen; Bedford, MA) or Alexa Fluor 750 (AF750) fluorophore (Invitrogen; Carlsbad, CA) per the manufacturer's instructions. This resulted in approximately 2 VT680 dyes or 3 AF750 dyes per antibody. There was no statistically significant change in Kd upon conjugation of the dyes as measured on HT-29 or A431 cells by flow cytometry. The dissociation of cetuximab was subnanomolar, and the Kd of the anti-EpCAM fluorophore conjugate was approximately 2 nM. Both these affinities were high enough that they should have a negligible impact on targeting based on simulations.

Cell Lines and Animal Model

For the mouse tumor xenografts, HT-29 human colon cancer cells were grown in McCoy's 5A media with 10% fetal bovine serum, 1% L-glutamine, 2% sodium bicarbonate, and 1% penicillin/streptomycin. Antigen expression levels were measured using quantitative beads (Bangs Laboratories; Fishers, IN) per the manufacturer's instructions. The reported values were measured in cell culture and verified in xenografts. For in vivo measurements, xenograft tumors were digested and measured as described previously[8] to verify that *in vivo* levels were similar to those measured *in vitro*. In addition, immunohistochemistry showed intense EpCAM staining in the HT-29 tumors whereas adjacent sections showed very low but still detectable EGFR staining (supplemental figure 1). Cells were diluted in PBS, and 50 uL containing ~1.5 million cells were injected subcutaneously in the back and flank of female nu/nu mice (Cox-7, Massachusetts General Hospital, Boston, MA). All animal experiments were carried out in accordance with guidelines from the Massachusetts General Hospital Subcommittee on Research Animal Care. Tumors grew to approximately 5 mm in diameter after 2 weeks when they were used for experiments. The actual time varied from 1 to 3 weeks in order to image tumors of the same size.

In vivo Experiments

Three days before imaging, mice were injected with 30 μg of anti-EpCAM and anti-EGFR antibody (unless stated otherwise for the text). This dose was large enough to give a significant signal relative to background autofluorescence but subsaturating according to the theoretical model. Saturating doses were calculated using the mathematical model[24] with the parameters listed in the tables. Experimental measurements were taken on 9 to 12 tumors in mice. Antibodies were dissolved in 100 μL of PBS and delivered by tail vein injection under isoflurane anesthesia. On the third day, the mice were anesthetized using 90 mg/kg ketamine and 10 mg/kg xylazine, the skin over the tumor and surrounding muscle was removed to reduce scattering, and the mice were imaged in an OV110 epifluorescence imaging system (Olympus; Center Valley, PA). The exposure time was set to 280 ms to use the dynamic range of the camera without saturating the images, and the gain was set to zero,

which gave linear intensity curves of standardized control wells filled with fluorescent dye. Image analysis was carried out using ImageJ (NIH) by drawing a region of interest around each tumor and taking the average intensity. Tumor to background ratios were calculated using the following equation:

$$TBR=(\text{Tumor signal}-\text{tumor autofluor.})/(\text{Background signal}-\text{background autofluor.})$$

where the autofluorescence signals were measured in uninjected mice. Means were compared using Student's T-test for statistical significance using Prism (GraphPad; La Jolla, CA).

To measure the plasma decay curves, blood samples were taken by retro-orbital puncture at multiple time points using heparin coated capillary tubes, imaged on the OV110 at high magnification, and compared to standards.

Results

A mathematical model capturing the transport steps of antibody uptake was used to simulate a tumor with varying antigen expression levels. Estimates for these parameters can be measured experimentally or taken from the literature[21]. Some of these parameters may vary depending on the model, such as the internalization rate. Using this parameter as an example, these rates often depend on the biology of the system, with clathrin coated pit uptake being faster than constitutive membrane turnover, which is faster than proteins associated with tight junctions[22,28]. Utilizing these estimates takes full advantage of the predictive capabilities of the model, while the parameters can be measured individually if the results differ significantly from predictions. With all other variables held constant (e.g. dose, antibody plasma clearance, antigen internalization rate, tumor vascularization, cell density, time after injection, etc.), the concentration of antibody in the tumor was plotted versus antigen concentration. At low expression levels, the concentration was proportional to the antigen expression level when all available binding sites were occupied (figure 1A). As the antigen expression goes to zero, the tumor concentration does not drop to zero but rather to a lower level as a result of non-specific poor extravasation and intravasation rates of macromolecules, often described as enhanced permeation and retention (EPR)[29]. At higher expression levels, the amount of antibody reaching the tumor was limited by extravasation across the vascular wall, and uptake concentrations plateaued. At this point, there were more available binding sites than antibodies that reached the tumor, and the concentration was dependent on delivery. Two fundamental dimensionless numbers describe when saturation is reached in the tumor, and both these numbers must be less than unity for saturation to occur[22].

To test the prediction that antigen expression level has a minimal impact on high affinity antibodies at subsaturating concentrations, two different antigens were targeted in the same tumor. Since the plateau concentration is highly dependent on tumor vascularization and permeability, which can vary widely between tumors, this allowed delivery to a highly expressed and moderately expressed target by the same vessels in the same tumor over an identical time period. The expression of epidermal growth factor (EGFR) and epithelial cell adhesion molecule (EpCAM) varies in magnitude in HT-29 human colon cancer cells. While EGFR is moderately expressed (38,000 EGFR/cell), EpCAM is highly expressed (2.3 million EpCAM/cell) as seen with flow cytometry and immunohistochemistry (supplemental). Even with this 50-fold difference in expression, a subsaturating dose of antibody is predicted to localize to a similar extent in both tumors (Figure 1B). This model

system was chosen since this constitutes one of the largest differences in expression where similar uptake can be demonstrated with fluorescent antibodies. (Antigens are rarely expressed at levels higher than several million antigens per cell, and it is difficult to achieve signals larger than background with cells expressing less than a few thousand targets.) The anti-EGFR antibody cetuximab conjugated to AF750 and an anti-EpCAM antibody conjugated to VT680 were injected via tail vein 3 days before imaging at a dose of 30 μg each per mouse. Although mouse antibodies are typically cleared more slowly than human antibodies in a mouse, the measured clearance (AUC) was similar for these two antibodies (supplemental). This is likely due to increased clearance of the mouse antibody in the liver and spleen of nude mice for this antibody isotype[30]. While the isotype can change the pharmacokinetics and pharmacodynamics (e.g. through FcRn and Fcγ receptor interactions), these antibodies were chosen since they resulted in a similar plasma area under the curve (AUC), which has a strong influence on uptake[5]. After removing the skin covering the tumor to reduce scattering, epifluorescence images were taken of the tumors. HT-29 cells grow as clusters of tumor cells surrounded by host macrophages and vasculature[8]. The uptake pattern of both antibodies in these cell clusters on the macroscopic scale was qualitatively similar (Figure 1C).

To quantify the uptake of these antibodies, region of interest analysis was done on all the tumors, and the average fluorescence intensity was measured. The intensity of both antibodies was similar in the first group of mice. However, image intensity is dependent on a large number of factors, including the intensity of the excitation light, filter specifications, fluorophore absorption and quantum efficiency, tissue scattering and absorption, and sensitivity of the camera to different wavelengths. To rule out effects based on the fluorophores, the fluorescent tags were switched and the experiment repeated. The intensities of the regions of interest were not significantly different between the two antibodies when labeled with the same probe even in different groups of mice (Figure 2).

Control experiments with a dilution series of the free dye resulted in 37.5 MFU/nM of VT680 dye and 33.3 MFU/nM of AF750 dye. Differences in tissue depth and scattering prevent precise quantification of concentrations, but these results indicate the antibody tumor concentrations are on the order of 50-100 nM and slightly higher for VT680 than AF750.

Theoretical models[8,24] indicate similar uptake between the two antibodies would be obtained at subsaturating doses. However, when one or both of the tumors are saturated, antibody uptake for the more highly expressed EpCAM is predicted to be higher than for EGFR. Using parameter estimates for the pertinent rates in uptake (table 1), it was possible to estimate the doses required for saturation. Using estimates of the Thiele modulus and Clearance modulus, it was calculated that a 5-fold increase in dose (150 μg dose) would still be subsaturating for the anti-EpCAM antibody but would saturate all the EGFR binding sites (table 2). In theory, a 150 μg blocking dose of non-fluorescent antibody (administered a day before the imaging dose of fluorescent antibody) should have no effect on the total uptake of anti-EpCAM antibody since there are still many free binding sites remaining. However, this same dose should bind all the EGFR in the tumor, reducing the amount of anti-EGFR uptake (Figure 3A). This same principle can be applied to humans, but the doses are much larger. Table 3 calculates typical doses needed to saturate a tumor in a 70-kg man with varying expression levels (supplemental).

Mice bearing HT-29 tumors identical to the first two groups were administered 150 μg of non-fluorescent anti-EGFR antibody and 150 μg of non-fluorescent anti-EpCAM antibody on day 1. On day 2, these mice received 30 μg of anti-EpCAM-VT680 and anti-EGFR-AF750, and three days after the fluorescent antibody (day 5), the mice were imaged. The

anti-EpCAM antibody yielded bright fluorescence in the clusters of tumor cells. However, the intensity of the anti-EGFR antibody was reduced, and the labeling pattern was different (Figure 3B). Rather than high uptake in the tumor cell clusters, the residual fluorescence was slightly more intense in the region surrounding the tumor clusters, a compartment previously shown to consist primarily of macrophages[8].

Quantifying the tumor to background ratio using region of interest analysis, the TBR did not change significantly for the anti-EpCAM antibody with or without a preblocking dose of non-fluorescent antibody. The TBR of the anti-EGFR antibody was significantly reduced, however, indicating a lack of free, accessible binding sites within the tumor (Figure 4).

During the subcutaneous injection of tumors, some cells often leak out along the needle track, forming small 'micrometastases.' Delivery to these small tumor clusters is better in theory due to their large surface area to volume ratios and diffusion from the surrounding normal tissue (Fig 5A). The concentration of IgG in normal tissue interstitium has been measured around 25-50% of that found in the plasma[31,32]. Uptake from the normal tissue is proportional to the tumor radius and antibody diffusion coefficient (D/R_{tumor}^2) rather than the permeability surface area product (PS/V) from antibody in the vessels. Localization of anti-EpCAM antibody in these small tumors is very high, consistent with significant delivery by the surrounding normal tissue. While delivery of the anti-EGFR antibody to the small tumor is presumably the same as anti-EpCAM antibody, the number of binding sites is far fewer, resulting in antibody diffusing back out of the metastasis and lower overall uptake (Figure 5B). Although the concentration of anti-EGFR antibody in the small tumor is predicted to be similar to anti-EGFR antibody in the large tumor, the much thicker large tumor gives a stronger signal intensity at similar concentrations. Simulations of a spherical tumor imbedded in normal tissue show a high but heterogeneous uptake of anti-EpCAM antibody around the tumor periphery, where the large number of binding sites immobilize the antibody near the surface. The fewer number of binding sites allows the anti-EGFR antibody to reach the center, albeit at a lower concentration. Some of this antibody is able to diffuse back out of the small tumor, and uptake is much lower in the saturated EGFR small tumor than with anti-EpCAM antibody (Figure 5C). This surface uptake becomes diminishingly important for tumors larger than about 1 mm (supplemental figure 2).

Discussion

Tumor targeting of antibodies is a complex process with many steps that have varying rates within and between tumors. Not surprisingly, given the diversity of tumor expression levels, antibody properties, and tumor types, some experimental results indicate a correlation between antibody uptake and antigen expression, while other papers report no correlation. By analyzing the fundamental steps in transport including blood flow, extravasation, diffusion, and binding relative to plasma clearance and local clearance from internalization, predictions can be made on the overall targeting and distribution of these antibodies. These theoretical models indicate that high affinity antibody uptake is not correlated with antigen expression unless all the binding sites in the tumor are occupied. This is especially important for the interpretation of imaging data, since signal intensity could wrongly be attributed to antigen expression levels depending on the experimental or clinical conditions.

The theoretical results can be explained based on the rates of antibody transport. The time scale for exchange of these macromolecules across the vascular wall is hours, but it only takes minutes to diffuse the distance between blood vessels and seconds to bind antigen[21]. Antibodies that extravasate out of the tumor vasculature therefore have time to diffuse to unbound antigen and associate before intravasating back into the blood. As long as there are free binding sites available in the tumor, these antibodies will be immobilized in the tissue.

Therefore, under subsaturating conditions, the localization of antibodies is limited by extravasation across the blood vessel wall. The anti-EGFR and anti-EpCAM antibodies localized to a similar extent in the HT-29 tumors even though their expression differed by over an order of magnitude. An alternative (but equally valid) conceptualization is that figure 1a represents an *in vivo* saturation curve. Given a constant dose and equal delivery (vascularization and permeability), a fixed amount of antibody reaches the tumor. As the number of antigens per cell increases, more of this antibody binds the target and is retained. Once the number of targets exceeds the number of antibodies that reach the tumor, the uptake is no longer dependent on the amount of antigen. This saturation curve is the reverse of what is typically done *in vitro*, where the antibody concentration is varied until a fixed amount of antigens (i.e. cells) are saturated.

It is important to note that despite the increased permeability of tumor blood vessels, the permeability still limits uptake of these macromolecules in tumors. The permeability of tumor blood vessels is high relative to normal vessels due to the effects of VEGF and other growth factors[33,34]. However, the rate at which antibodies cross the blood vessel wall (the permeability) is low relative to the other steps in targeting (tumor blood flow, interstitial diffusion, and binding) implicating the permeability as the rate limiting step in uptake. These relative rates emphasize the need for quantitative models to describe uptake, since statements on ‘high’ and ‘low’ permeability are context dependent. Even though the signal is limited by delivery at subsaturating concentrations, it is still antigen dependent. The lower uptake of a non-binding antibody (or tumor that lacks binding sites) is often used to show specificity. Using a functional definition of saturation, where saturation is the lack of accessible, unoccupied binding sites in the tumor, a non-binding antibody is always ‘saturated.’ This runs counter to traditional thinking where this type of antibody would never saturate a tumor, but it agrees with the theoretical and experimental results. The Thiele modulus and clearance modulus, which must be less than one for saturation, are identically zero with no antigen. As the antigen concentration approaches zero in figure 1a, the antibody concentration approaches the EPR level of a non-binding antibody. Experimentally, the anti-EGFR antibody in figure 3b distributed similar to a non-binding antibody injected in these tumors (supplemental figure 3). Both of these antibodies in the ‘saturated’ regime lacked free accessible binding sites.

Using a theoretical model of tumor saturation, the saturating dose of antibody was calculated for both antigens in these tumors. By choosing a dose in between the levels for these antibodies, the lower expression antigen was saturated while the higher expressing antigen retained free binding sites. This demonstrates the quantitative nature of the model, since too low of a dose wouldn't affect either antigen, while too high of a dose would affect both antigens. In order to saturate a highly expressed antigen, a much larger dose is needed. To saturate EGFR on A431 cells that express several million receptors per cell, Li et al. used a 1 mg dose of antibody per mouse to block the sites and reduce uptake[1]. Similarly, McLarty et al. used a 0.8 mg dose to saturate HER2 expressed at half a million receptors per cell. The corollary is presented in this paper, where a 0.15 mg dose was not sufficient to saturate EpCAM in HT-29 cells. Localization of the anti-EGFR antibody was reduced when the mice received a saturating dose; however, the tumor to background ratio was still above two. Some of this uptake may be from the high rates of permeability and lack of efficient lymphatic drainage in the tumor (the enhanced permeability and retention, or EPR effect). Based on the overall distribution of this antibody, a fraction also colocalizes with macrophages in the stromal tissue and surrounding tumor capsule. The relative contribution of fluid phase uptake or binding to Fc receptors on the surface of these cells is not known.

There were some fluorophore specific effects on signal concentration in the tumors studied here. Although the different antigen internalization rates were accounted for in the model

(table 1), the cellular loss of the tag can dominate the loss of signal if this is much slower than the internalization rate (supplemental section 7). Estimating tumor concentrations based on the number of fluorophores per antibody and the signal intensity from calibrated control solutions, the concentration of VT680 fluorophore was double to triple that of the AF750 fluorophore, independent of the antibody used for localization. While the precise mechanism for this difference is not known, *in vitro* experiments indicate that the VT680 dye is trapped within the cells for a longer period of time following internalization (data not shown). Similar to the residualizing nature of some radioisotopes, fluorophores that are trapped inside cells for longer times will yield a higher signal[35]. Antibodies labeled with indium-111, for example, give a higher signal than those labeled with iodine, which is able to escape cells at a faster rate following internalization and catabolism[36]. Since background signal is likely from free antibody while the tumor signal contains a significant portion of internalized and degraded antibody, the cellular retention rate preferentially affects the tumor signal over background. This mechanism is consistent with the higher tumor to background ratios found with VT680 labeled antibodies over AF750 labeled antibodies in figure 4 and explains why the model is not very sensitive to the different antigen internalization rates in these experiments.

These results help clarify differences in correlations between uptake and antigen expression in the literature. With low extravasation rates in tumors relative to the number of binding sites, subsaturating doses of antibody are often used with imaging. In these instances, uptake is not proportional to expression level but related to delivery by the vasculature[20,37]. The number of binding sites of a particular antigen can vary by orders of magnitude, with some of the highest expressing cells containing several million binding sites per cell. However, other lines express much lower levels, and if these targets are chosen, saturating doses can more easily be achieved. Cai et al. showed a linear correlation between expression levels and uptake, possibly indicating some of these tumors were saturated.

An important paper by McLarty et al.[17] used several cell lines with varying HER2 expression to measure uptake as a function of antigen density. Their results showed an overall non-linear uptake curve as a function of antigen density. Their experimental data look similar to the theoretical trend in figure 1a of this paper, demonstrating a near linear correlation at low expression levels but little dependence at high expression levels. To obtain this curve, the authors had to normalize their data to uptake of a non-specific antibody, effectively normalizing the variable delivery (vascularization and permeability) between the different cell lines. To make a more robust comparison of our model predictions to experimental data with variable target expression, we not only used the same cell line (which could have been achieved by varying transfection levels) but also the same tumor. This eliminates any inter-tumor differences in vascularization, permeability, blood flow, diffusion, etc. and enables multichannel imaging of targeted antigens with high and low expression in a single tumor. Therefore, we were required to choose different targets in the tumor. Neither experiments with different cell lines and tumors or with different antibodies can completely isolate the effects of antigen expression, which is why theoretical modeling is imperative. However, both studies using the same antibody and different tumors[17] and the current data with the same tumor and different antibodies are consistent with the model predictions.

For human studies, the model predicts very large doses are required for saturation, on the order of hundreds of milligrams to grams (table 3). These values were obtained using estimates of biological parameters or values (such as antigen expression and plasma clearance) measured in the clinic. With therapeutic antibodies, doses are given repeatedly maintaining an elevated plasma level over an extended period of time, but several mg/kg are required to overcome the slow extravasation and catabolism in tumor tissue. In general,

these doses are high enough for saturation. Imaging agents are given as a single dose, and saturation is not necessary for sufficient tumor to background ratios. For radiolabeled antibodies, doses are well below saturation, and even optical agents such as for FILM are not saturating in most scenarios. Under these conditions, overall uptake in the tumor is not related to antigen expression.

Important information can be obtained from the small tumors along the needle track. There are multiple mechanisms for higher uptake near the surface of tumors. Since the local vascular surface area determines the delivery to a particular region, large tumors with central necrosis will have little antibody in their center[38,39]. There is also the possibility of higher effective permeability in vessels near the surface due to lower interstitial pressure in this region[40]. Both these mechanisms require vascularized tumors, however, and it does not appear there are any vessels in the 500-700 um diameter tumor in Figure 5. Uptake in this tumor results from diffusion from the surrounding normal tissue. The large number of binding sites immobilizes the antibody at the surface, and over time the binding site front moves towards the center[23]. With lower expression levels of EGFR, the metastasis was saturated with this antibody. The absolute number of binding sites in this small lesion is low and difficult to visualize against the background autofluorescence, which is highly relevant in tumor targeting for surgical resection. The same distribution pattern is expected around the blood vessels in the large tumor, with the high expression levels immobilizing the anti-EpCAM antibody in a perivascular distribution while the anti-EGFR is able to penetrate farther away from the vessels due to fewer binding sites in the tissue. The scattering of the tissue prevents this from being seen by epifluorescence in the large tumors, but qualitatively, the distribution of the anti-EpCAM antibody is more punctate near the surface with the anti-EGFR antibody resulting in more diffuse localization (supplemental figure 4).

It is important to note that these results are valid for high affinity antibodies. Lower affinity antibodies have a larger fraction unbound in the tumor, allowing them to intravasate at a rate depending on the local antigen concentration. This assumption is not as limiting as it first appears. Since IgG molecules are bivalent, even if the intrinsic affinity is low, the valency often causes rebinding before the molecule completely dissociates, so it functions as a high affinity antibody[41].

These results have important implications for therapy and imaging. For therapy, this indicates these smaller metastases are more easily targeted than vascularized tumors. This is an additional but distinct mechanism (diffusion from the metastasis surface) from other size dependencies, such as the extent of vascularization[42]. For imaging applications such as fluorescent intraoperative live microscopy[8], the expression level will determine the size of tumors that are visible. While moderate expression is sufficient to detect larger tumors (e.g. several mm to cm in diameter) for surgical debulking[43], high expression is required to detect smaller micrometastatic deposits such as the small lesion in figure 5 for complete resection. The saturation doses in table 3 are similar to therapeutic doses used in the clinic but are impractically large for nuclear medicine imaging applications where the smallest possible dose is often desired. To circumvent this problem, either therapies must be able to reduce the expression level until the imaging agent is capable of saturating the antigen for measurements[3,44] or other mechanisms of quantification must be developed. This experimental demonstration of the theoretical predictions support the use of quantitative modeling in the design of more efficacious treatments[25] and timely quantitative imaging agents.

Supplementary Material

Refer to Web version on PubMed Central for supplementary material.

Acknowledgments

This work was supported by grants P50 CA86355, U24 CA092782, and T32 CA079443.

Abbreviations

EGFR	Epidermal Growth Factor Receptor
EpCAM	Epithelial Cell Adhesion Molecule
VT680	VivoTag 680 fluorescent dye
AF750	AlexaFluor 750 fluorescent dye

References

1. Li WP, Meyer LA, Capretto DA, Sherman CD, Anderson CJ. Receptor-binding, biodistribution, and metabolism studies of Cu-64-DOTA-cetuximab, a PET-imaging agent for epidermal growth-factor receptor-positive tumors. Cancer Biother Radiopharm. 2008; 23:158–171. [PubMed: 18454685]
2. Zhao BS, Schwartz LH, Larson SM. Imaging Surrogates of Tumor Response to Therapy: Anatomic and Functional Biomarkers. Journal of Nuclear Medicine. 2009; 50:239–249. [PubMed: 19164218]
3. McLarty K, Cornelissen B, Cai ZL, Scollard DA, Costantini DL, Done SJ, Reilly RM. Micro-SPECT/CT with In-111-DTPA-Pertuzumab Sensitively Detects Trastuzumab-Mediated HER2 Downregulation and Tumor Response in Athymic Mice Bearing MDA-MB-361 Human Breast Cancer Xenografts. Journal of Nuclear Medicine. 2009; 50:1340–1348. [PubMed: 19617342]
4. Zhang YJ, Xiang LM, Hassan R, Pastan I. Immunotoxin and Taxol synergy results from a decrease in shed mesothelin levels in the extracellular space of tumors. Proc Natl Acad Sci U S A. 2007; 104:17099–17104. [PubMed: 17940013]
5. Wu AM, Senter PD. Arming antibodies: prospects and challenges for immunoconjugates. Nature Biotechnology. 2005; 23:1137–1146.
6. Sharkey RM, Karacay H, Cardillo TM, Chang CH, McBride WJ, Rossi EA, Horak ID, Goldenberg DM. Improving the delivery of radionuclides for imaging and therapy of cancer using pretargeting methods. Clinical Cancer Research. 2005; 11:7109S–7121S. [PubMed: 16203810]
7. Mattes MJ, Sharkey RM, Karacay H, Czuczman MS, Goldenberg DM. Therapy of Advanced B-Lymphoma Xenografts with a Combination of Y-90-anti-CD22 IgG (Epratuzumab) and Unlabeled Anti-CD20 IgG (Veltuzumab). Clin Cancer Res. 2008; 14:6154–6160. [PubMed: 18829494]
8. Thurber G, Figueiredo J, Weissleder R. Multicolor Fluorescent Intravital Live Microscopy (FILM) for Surgical Tumor Resection in a Mouse Xenograft Model. PLoS ONE. 2009; 4:e8053. [PubMed: 19956597]
9. Zou P, Xu SB, Povoski SP, Wang A, Johnson MA, Martin EW, Subramaniam V, Xu R, Sun DX. Near-infrared Fluorescence Labeled Anti-TAG-72 Monoclonal Antibodies for Tumor Imaging in Colorectal Cancer Xenograft Mice. Molecular Pharmaceutics. 2009; 6:428–440. [PubMed: 19718796]
10. Urano Y, Asanuma D, Hama Y, Koyama Y, Barrett T, Kamiya M, Nagano T, Watanabe T, Hasegawa A, Choyke PL, et al. Selective molecular imaging of viable cancer cells with pH-activatable fluorescence probes. Nature Medicine. 2009; 15:104–109.
11. Rosenthal EL, Kulbersh BD, King T, Chaudhuri TR, Zinn KR. Use of fluorescent labeled anti-epidermal growth factor receptor antibody to image head and neck squamous cell carcinoma xenografts. Mol Cancer Ther. 2007; 6:1230–1238. [PubMed: 17431103]
12. Jayson GC, Zweit J, Jackson A, Mulatero C, Julyan P, Ranson M, Broughton L, Wagstaff J, Hakannson L, Groenewegen G, et al. Molecular imaging and biological evaluation of HuMV833 anti-VEGF antibody: Implications for trial design of antiangiogenic antibodies. J Natl Cancer Inst. 2002; 94:1484–1493. [PubMed: 12359857]
13. Stollman TH, Scheer MGW, Franssen GM, Verrijp KN, Oyen WJG, Ruers TJM, Leenders WPJ, Boerman OC. Tumor Accumulation of Radiolabeled Bevacizumab due to Targeting of Cell- and

Matrix-Associated VEGF-A Isoforms. Cancer Biother Radiopharm. 2009; 24:195–200. [PubMed: 19409041]

14. Wu AM, Olafsen T. Antibodies for molecular imaging of cancer. Cancer J. 2008; 14:191–197. [PubMed: 18536559]
15. Smith-Jones PM, Solit D, Afroze F, Rosen N, Larson SM. Early tumor response to Hsp90 therapy using HER2 PET: Comparison with F-18-FDG PET. Journal of Nuclear Medicine. 2006; 47:793–796. [PubMed: 16644749]
16. Cai WB, Chen K, He LN, Cao QH, Koong A, Chen XY. Quantitative PET of EGFR expression in xenograft-bearing mice using Cu-64-labeled cetuximab, a chimeric anti-EGFR monoclonal antibody. Eur J Nucl Med Mol Imaging. 2007; 34:850–858. [PubMed: 17262214]
17. McLarty K, Cornelissen B, Scollard DA, Done SJ, Chun K, Reilly RM. Associations between the uptake of In-111-DTPA-trastuzumab, HER2 density and response to trastuzumab (Herceptin) in athymic mice bearing subcutaneous human tumour xenografts. Eur J Nucl Med Mol Imaging. 2009; 36:81–93. [PubMed: 18712381]
18. Aerts H, Dubois L, Perk L, Vermaelen P, van Dongen G, Wouters BG, Lambin P. Disparity Between In Vivo EGFR Expression and Zr-89-Labeled Cetuximab Uptake Assessed with PET. Journal of Nuclear Medicine. 2009; 50:123–131. [PubMed: 19091906]
19. Milenic DE, Wong KJ, Baidoo KE, Ray GL, Garmestani K, Williams M, Brechbiel MW. Cetuximab: Preclinical Evaluation of a Monoclonal Antibody Targeting EGFR for Radioimmunodiagnostic and Radioimmunotherapeutic Applications. Cancer Biother Radiopharm. 2008; 23:619–631. [PubMed: 18999934]
20. Niu G, Li Z, Xie J, Le QT, Chen X. PET of EGFR antibody distribution in head and neck squamous cell carcinoma models. J Nucl Med. 2009; 50:1116–1123. [PubMed: 19525473]
21. Thurber G, Schmidt M, Wittrup KD. Factors determining antibody distribution in tumors. Trends in Pharmacological Sciences. 2008; 29:57–61. [PubMed: 18179828]
22. Thurber GM, Schmidt MM, Wittrup KD. Antibody tumor penetration: Transport opposed by systemic and antigen-mediated clearance. Adv Drug Deliv Rev. 2008; 60:1421–1434. [PubMed: 18541331]
23. Thurber GM, Wittrup KD. Quantitative spatiotemporal analysis of antibody fragment diffusion and endocytic consumption in tumor spheroids. Cancer Research. 2008; 68:3334–3341. [PubMed: 18451160]
24. Thurber GM, Zajic SC, Wittrup KD. Theoretic criteria for antibody penetration into solid tumors and micrometastases. J Nucl Med. 2007; 48:995–999. [PubMed: 17504872]
25. Schmidt MM, Wittrup KD. A modeling analysis of the effects of molecular size and binding affinity on tumor targeting. Mol Cancer Ther. 2009; 8:2861. [PubMed: 19825804]
26. Mager DE. Target-mediated drug disposition and dynamics. Biochemical Pharmacology. 2006; 72:1–10. [PubMed: 16469301]
27. Adams G, Schier R, McCall A, Simmons H, Horak E, Alpaugh K, Marks J, Weiner L. High Affinity Restricts the Localization and Tumor Penetration of Single-Chain Fv Antibody Molecules. Cancer Research. 2001; 61:4750–4755. [PubMed: 11406547]
28. Ackerman ME, Chalouni C, Schmidt MM, Raman VV, Ritter G, Old LJ, Mellman I, Wittrup KD. A33 antigen displays persistent surface expression. Cancer Immunol Immunother. 2008; 57:1017–1027. [PubMed: 18236042]
29. Noguchi Y, Wu J, Duncan R, Strohalm J, Ulbrich K, Akaike T, Maeda H. Early phase tumor accumulation of macromolecules: a great difference in clearance rate between tumor and normal tissues. Japanese Journal of Cancer Research. 1998; 89:307–314. [PubMed: 9600125]
30. Sharkey RM, Natale A, Goldenberg DM, Mattes MJ. Rapid Blood Clearance of Immunoglobulin-G2A and Immunoglobulin-G2B in Nude-Mice. Cancer Res. 1991; 51:3102–3107. [PubMed: 2039990]
31. Lonsmann H. Interstitial fluid concentrations of albumin and immunoglobulin-G in normal men. Scand J Clin Lab Invest. 1974; 34:119–122. [PubMed: 4424039]
32. Wiig H, Gyenge CC, Tenstad O. The interstitial distribution of macromolecules in rat tumours is influenced by the negatively charged matrix components. J Physiol -London. 2005; 567:557–567. [PubMed: 15994186]

33. Weis SM, Cheresh DA. Pathophysiological consequences of VEGF-induced vascular permeability. 2005; 437:497–504.
34. Yuan F, Chen Y, Dellian M, Safabakhsh N, Ferrara N, Jain RK. Time-dependent vascular regression and permeability changes in established human tumor xenografts induced by an anti-vascular endothelial growth factor vascular permeability factor antibody. Proc Natl Acad Sci U S A. 1996; 93:14765–14770. [PubMed: 8962129]
35. Maxwell JL, Terracio L, Borg TK, Baynes JW, Thorpe SR. A Fluorescent Residualizing Label for Studies on Protein-Uptake and Catabolism Invivo and Invitro. 1990; 267:155–162.
36. Ferl GZ, Kenanova V, Wu AM, DiStefano JJ. A two-tiered physiologically based model for dually labeled single-chain Fv-Fc antibody fragments. 2006; 5:1550–1558.
37. Sung C, Youle RJ, Dedrick RL. Pharmacokinetic Analysis of Immunotoxin Uptake in Solid Tumors - Role of Plasma Kinetics, Capillary-Permeability, and Binding. Cancer Research. 1990; 50:7382–7392. [PubMed: 2224866]
38. Ahlstrom H, Christofferson R, Lorelius L. Vascularization of the continuous human colonic cancer cell line LS 174 T deposited subcutaneously in nude rats. APMIS. 1988; 96:701–710. [PubMed: 3415845]
39. Flynn A, Boxer G, Begent R, Pedley R. Relationship between tumour morphology, antigen and antibody distribution measured by fusion of digital phosphor and photographic images. Cancer Immunology and immunotherapy. 2001; 50:77–81. [PubMed: 11401028]
40. Baxter L, Jain RK. Transport of Fluid and Macromolecules in Tumors: 1. Role of Interstitial Pressure and Convection. Microvascular Research. 1989; 37:77–104. [PubMed: 2646512]
41. Tang Y, Lou J, Alpaugh RK, Robinson MK, Marks JD, Weiner LM. Regulation of antibody-dependent cellular cytotoxicity by IgG intrinsic and apparent affinity for target antigen. 2007; 179:2815–2823.
42. Hilmas D, Gillette E. Morphometric Analyses of the Microvasculature of Tumors During Growth and After X-Irradiation. Cancer. 1974; 33:103–110. [PubMed: 4810083]
43. Hoskins WJ, McGuire WP, Brady MF, Homesley HD, Creasman WT, Berman M, Ball H, and Berek JS (1994) (Mosby-Year Book Inc), pp. 974-980.
44. Smith-Jones PM, Solit DB, Akhurst T, Afroze F, Rosen N, Larson SM. Imaging the pharmacodynamics of HER2 degradation in response to Hsp90 inhibitors. Nat Biotechnol. 2004; 22:701–706. [PubMed: 15133471]

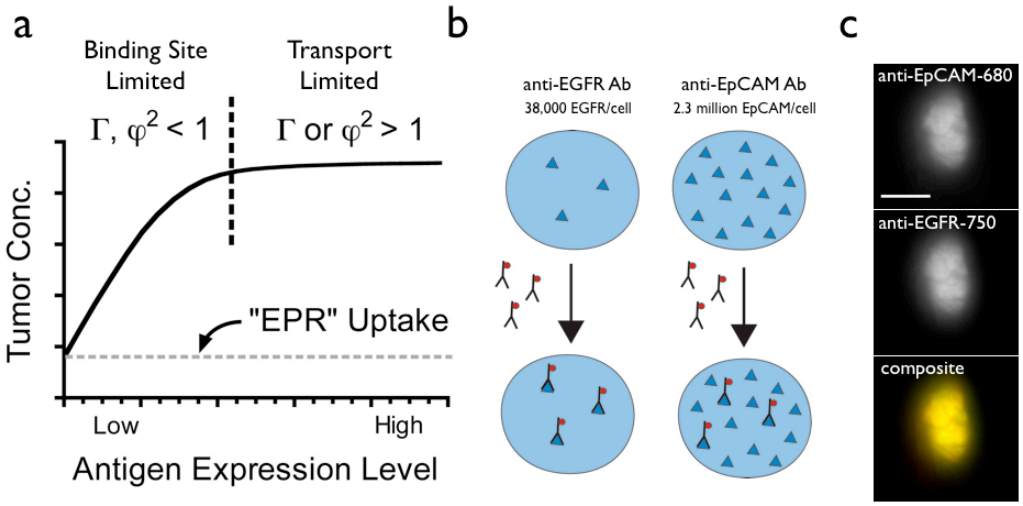

Figure 1.

Effect of antigen expression on uptake. When the Clearance modulus and Thiele modulus are less than 1, the tumor concentration is a function of the antigen expression level. At subsaturating concentrations, the uptake is a function of transport to the tumor (A). Targeting of antibodies is similar between moderately expressed EGFR and highly expressed EpCAM at subsaturating concentrations (B). Image of a tumor targeted by anti-EpCAM and anti-EGFR antibodies showing qualitatively similar uptake (C). Scale bar = 5 mm

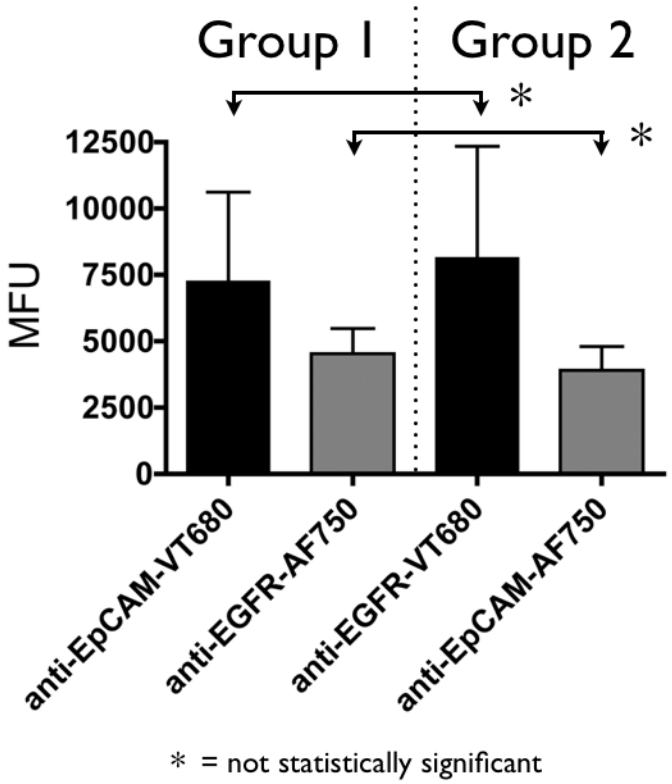

Figure 2.
Quantifying antibody uptake. The fluorescence intensity between anti-EpCAM and anti-EGFR antibodies is similar with the effects of the fluorophore accounting for most of the difference.

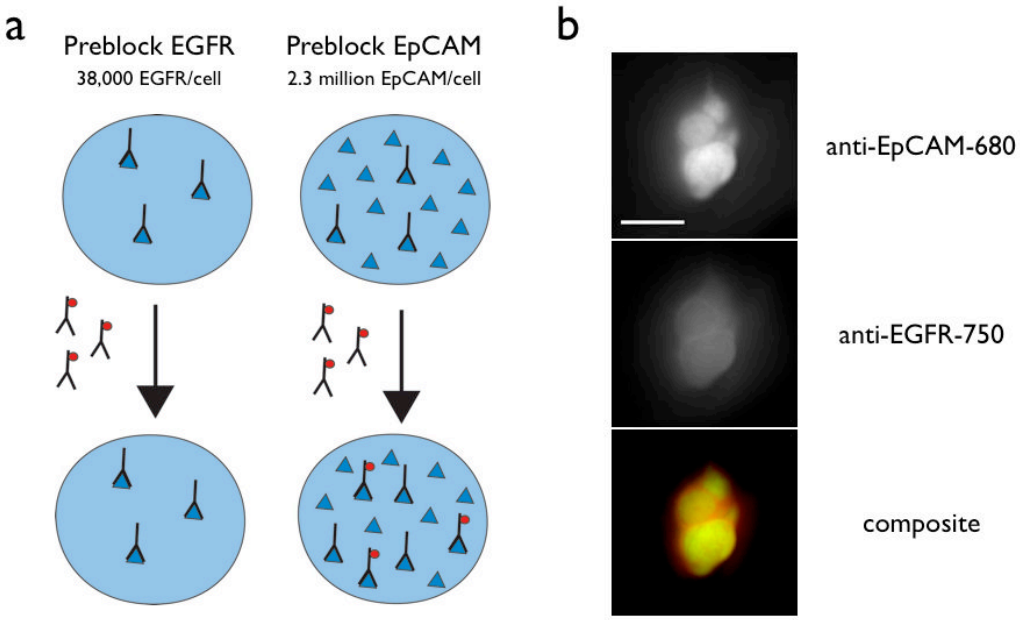

Figure 3.

Effect of saturating antigen with a non-fluorescent blocking antibody. A blocking dose that saturates EGFR but not EpCAM will lower uptake of anti-EGFR antibodies but not the anti-EpCAM antibodies (A). Mice given 150 μg doses of anti-EGFR and anti-EpCAM antibodies before administration of fluorescent antibodies had little effect on targeting of the EpCAM antibody but significantly lowered the uptake of anti-EGFR antibodies (B). Scale bar = 5 mm

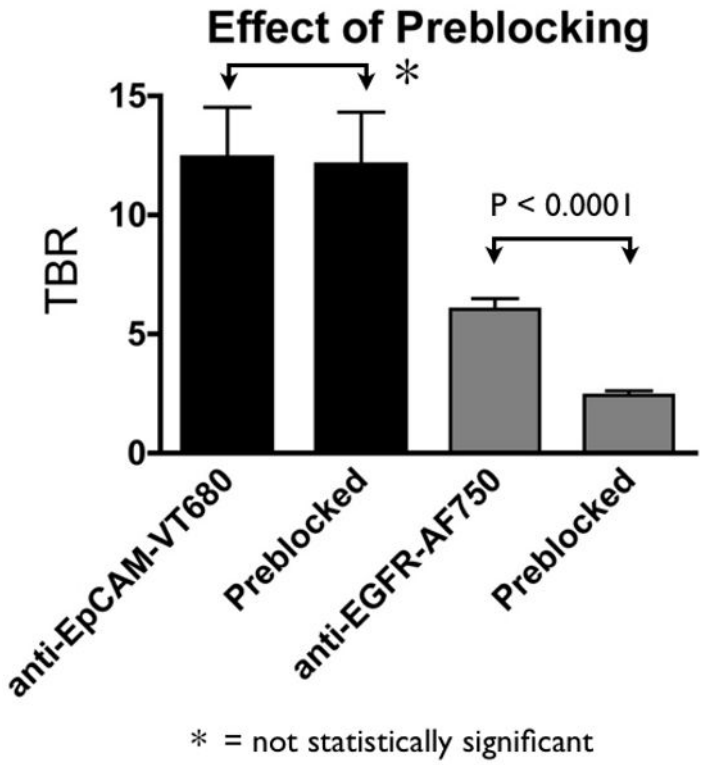

Figure 4.
Quantifying antibody uptake after preblocking the antigen. The targeting of the EpCAM antibody was not affected by the blocking dose, but the EGFR antibody had significantly lower uptake.

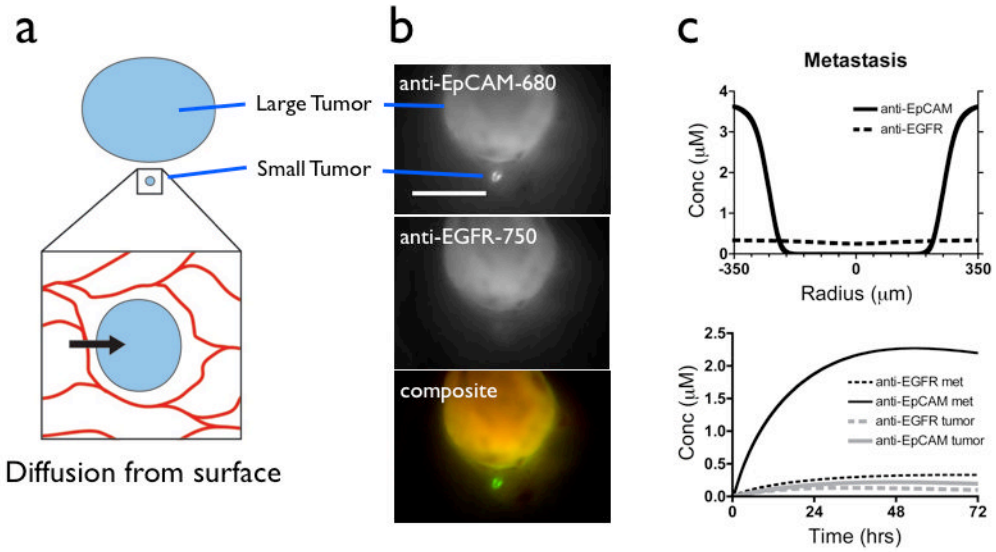

Figure 5.

Targeting micrometastases and small tumors. Antibody diffusing inward from the surrounding normal tissue targets a larger fraction of a small tumor (A). Significant uptake of anti-EpCAM antibody and saturation of the EGFR in a small metastasis (B). Scale bar = 5 mm. Mathematical model of uptake in a small prevascular metastasis. The large number of binding sites immobilizes the EpCAM antibody in the periphery, while the few EGFR binding sites are saturated at a low level (C, top). The overall concentration of EpCAM antibody in the small metastasis is higher than EpCAM antibody in the large tumor due to the high surface area to tumor volume of the metastasis (C, bottom).

Table 1

Model parameters

Parameter	Value
EpCAM/cell	2,300,000 (1900 nM)
EGFR/cell	38,000 (32 nM)
P	3×10^{-9} m/s
S/V	100/cm
clearance	mouse = 2.8×10^{-6}/s human = 4.9×10^{-6}/s
EpCAM internalization	1.3×10^{-5}/s half life ~ 15 hr
EGFR internalization	1.9×10^{-4}/s
	half life ~ 1 hr
dose	100 nM, 500 nM
Thiele modulus	$\frac{k_e[Ag]V}{PS[Ab]}$
Clearance modulus	$\frac{[Ag]V}{PS[Ab]\left(\frac{A}{k_\alpha}+\frac{B}{k_\beta}\right)}$

Table 2

Calculated Thiele modulus and Clearance modulus for Imaging and Preblocking Doses

Antigen	Experiment	Thiele	Clearance	Prediction
EpCAM	imaging Ab only	8.2	1.8	unsaturated
	preblock	1.6	0.4	unsaturated
EGFR	imaging Ab only	2.0	0.05	unsaturated
	preblock	**0.4**	**0.01**	**saturated**

Both Thiele and Clearance modulus < 1 for saturated.

Table 3

Saturating Doses in a 70 kg man

Expression (receptors/cell)	Amount needed to saturat tumor burden			Typical clinical doses		
	highly vascularized	moderately vascularized	poorly vascularized/necrotic	Tx	PET	FILM
High (10^6)	250 mg	1000 mg	> 5000 mg	1000 mg	1-10 mg	100 mg
Moderate (10^5)	25 mg	100 mg	> 500 mg			
Low (10^4)	3 mg	10 mg	> 50 mg			

Doses are in mg per 70 kg patient

Saturation doses assume linear kinetics (no tumor mediated drug disposition)

Doses are independent of tumor burden, although larger tumors are generally less well vascularized